

Tapered Fibre Optic Biosensor (TFOBS) by Optically Controlled Etching for Label-Free Glucose Concentration Monitoring

Biomedical Optics

Sergio Mena, Maria Morant, Juan Hurtado and Roberto Llorente

Nanophotonics Technology Center, Universitat Politècnica de València, Camino de Vera s/n, Valencia, Spain

Keywords: TFOBS, Glucose Sensing, Label-Free, Optical Sensor, Chemical Etching, Biconical Taper, Refractive Index, Optically Controlled Etching.

Abstract: This paper proposes, designs and demonstrates experimentally a tapered fibre optic biosensor (TFOBS) fabricated by an optically controlled HF chemical etching. The fabricated device is demonstrated to operate properly as a label-free sensor for glucose concentration detection. This work presents a novel fabrication method of a single-mode TFOBS controlling the reaction rate by changing the HF concentration and monitoring the optical power variation at the fibre output. Two TFOBS fabricated with different cladding diameters are evaluated experimentally to sense different glucose concentrations observing the changes in the refractive index of the medium in various solvents. The sensing capabilities are evaluated by modal interferometry measurement of both intensity and phase variations of the received optical signal.

1 INTRODUCTION

Glucose ($C_6H_{12}O_6$) is one of the most abundant organic compound in the human body, being part of a large number of macromolecules with structural importance. The singularity of this molecule comes from its capability of providing cellular energy. The presence of glucose in blood enables the energetic cell's sustenance, but it is also present in other biofluids such as urine, tears and sweat. The concentration control of glucose is of vital importance in patients with diabetes mellitus, whose amount increases every year (World Health Organization, 2016), for the maintenance of homeostasis and the regulation of insulin application. At present, most common commercial methods to measure glucose concentration are based on amperometric sensing measuring the reaction of glucose oxidase (GOx) with the glucose (Ferri et al., 2011). The amperometric sensing method is specific only for glucose detection and enables low-levels detection but has some disadvantages, such as:

- Complicated adaptation to continuous measurement.
- Electrical interference in biological fluids.
- Specificity affected by other oxidizing substances.

Due to the limitations of electrochemical sensors, optical biosensing has been appointed as a good solution to measure different biological elements such as Botulinum Neurotoxin (Guo et al., 2011) or Ammonia (Ruan et al., 2008). In fibre optic biosensors, the optical fibre is employed as a transduction media in order to produce or detect a signal proportional to the concentration of the biological element to sense (Bosch et al., 2007). Among other optical sensor types, tapered optical fibre sensors enables the exposure of evanescent field (EF) beyond the surface of the sensing region (Fielding and Davis, 2002). These systems are known as tapered fibre optic biosensors (TFOBS) and enable label-free detection (Leung et al., 2008a), reduced sample size and real-time response at a reduced size and low price (Qiu et al., 2015). In the last years, several TFOBS studies have been performed comparing single-mode and multimode fibre sensors, pointing out that multimode fibre sensor are less efficient due to a lower average electric field at the surface of the fibre compared with single-mode fibres (Fielding and Davis, 2002).

More complex sensors have been developed in the last years, such as graphene-based sensors (Qiu et al., 2015) and antibody-immobilized protein sensors (Leung et al., 2008b). The simplicity of TFOBS resides on the suitability of optical fibre media to

radiate the evanescent waves travelling through the fibre to the outside to interact with the sample to be detected (Qiang et al., 2014). A tapered fibre is produced by reducing gradually the diameter of a common optical fibre, which enables the interaction of the evanescent field guided in the fibre with the external environment (Baude and Branco, 2013). There are two main techniques for the fabrication of tapered fibre: (i) by chemical or mechanical corrosion of the fibre cladding (Ruan et al., 2008; Bal et al., 2012) or (ii) by simultaneous heating and stretching of the fibre (Kenny et al., 1991). The main differences between both techniques resides in the resulting core diameter. In the first case, implementing corrosion of the cladding, the fibre core remains the same (i.e. 8.2 μm in single-mode fibre SMF-28). While, in the second case, by heating and stretching, the diameter of both the cladding and the core is reduced in the same proportion (Kenny et al., 1991). In this work, a simple method to produce the EF on a single-mode fibre by cladding corrosion is described, producing a tapered fibre with hydrofluoric acid etching (Haddock et al., 2003). This approach provides better light transmission due to the no degradation of the fibre core (Bal et al., 2012). The resulting tapered fibre can be used as an optical biosensor and is an affordable solution for glucose monitoring.

This paper is structured as follows: in section 2 the laboratory steps for the fabrication of the tapered optical fibre are described in detail. A novel fabrication method of TFOBS is proposed controlling the reaction rate by changing the HF concentration and monitoring the optical power variation at the fibre output. Next, in section 3 of this work, we evaluate experimentally the sensing method based on modal interferometry for different concentrations. Finally, in section 4, the main conclusions of this work and the consideration of future implementations are reported.

2 OPTICALLY CONTROLLED CHEMICAL ETCHING TAPERED FIBRE FABRICATION

The novelty of the proposed fabrication method resides in performing the chemical etching at a controlled rate. There are two different approaches for monitoring the chemical etching process. The first one employs an optical system (e.g a microscope or magnifying glass) to measure in real-time the waist diameter while the chemical etching is performed.

However, this method is not appropriate for chemical etching employing hydrofluoric (HF) acid for security reasons. The second approach is based on monitoring the pass-through optical power, using an optical light source and a potentiometer, and correlating the power loss with the diameter of the optical fibre in the reaction length. This approach is implemented following the experimental setup depicted in Figure 1.

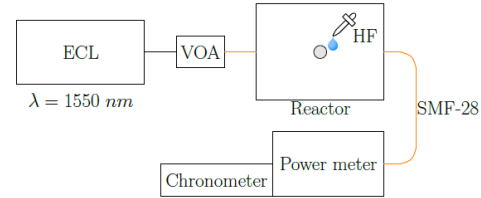
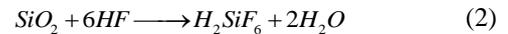
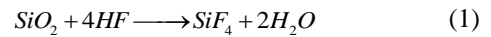


Figure 1: Laboratory setup for optically controlled HF acid chemical etching.

In this experimental demonstration an external cavity laser (ECL) operating at $\lambda = 1549.65 \text{ nm}$ (Ando AQ8201-13B) is employed. A variable optical attenuator (VOA) is used to reduce the optical power level at the input of the SMF-28 reactor to avoid a possible fibre break. The chemical etching is performed using a HF solution of 49.5 wt% to be neutralized with NaOH solutions of 0.1 M and 5 M. An optical power meter and a chronometer are used to measure the evolution of optical power level passing through the tapered fibre with time.

When the HF come into contact with the SiO_2 of the optical fibre, the resulting chemical reactions are defined in Equation 1 and Equation 2. When the HF acid has a high concentration, the second reaction is prevailing (Abbadie et al., 2007), which makes it easier to obtain a mathematical model of the reaction process:



The mathematical expressions for the chemical reaction are included in Equation 3 and Equation 4 (Haddock et al., 2003), where D_i and D_f are the initial and final diameters of the fibre, respectively, C and Z are constant values, t is the reaction time, $[\text{HF}]$ is the acid concentration, k is the reaction constant, r is the density of the silica, P is the received optical power level and L is the length of the fibre in contact with the acid.

$$\frac{D_f}{D_i} = C - Kt, \quad K = \frac{2k[\text{HF}]}{D_f \rho} \quad (3)$$

$$P \propto D^2 L \leftrightarrow P = ZD^2 L \quad (4)$$

The K parameter groups the constant parameters of the Equation 3. As a result of Equation 3 and Equation 4, we obtain the linear relation expressed in Equation 5:

$$\sqrt{\frac{P_f}{P_i}} = C - Kt \quad (5)$$

With these equations it is possible to have a first calculation of the necessary reaction time in order to reach the desired diameter of the fibre for the TFOBS. Next, using a simple experimental setup as depicted in Figure 1, the optical power level can be monitored to confirm if the chemical reaction is done properly and to determine when to neutralize and stop the reaction. However, some aspects should be taken into account:

- The reaction variable K of the mathematical model is constant as long as the environmental conditions are stable (i.e. room temperature, lighting...)
- The relation between the diameter and the received power is accurate when D_f approaches the core diameter, as the optical signal is mainly transmitted through the core. Thus, the linear relation depicted in Equation 5 is valid when the received optical power starts decreasing.

In this work, the objective is to obtain, from a SMF-28 fibre with 125 μm diameter cladding, a biconical structure with a reduced cladding of 15 μm for TFOBS implementation. Table 1 includes the monitoring parameters obtained using the mathematical model. The K value is obtained from 20 essays under standard conditions according to (Haddock et al., 2003). The volume of HF acid used is 75 μL , of which only about 0.8% will react, making the etching process rate approximately constant.

Table 1: Monitoring parameters of the chemical etching.

$K(s^{-1})$	$\frac{P_a}{P_i}$	$t(s)$
$2.3 \cdot 10^{-3} \pm 1.9 \cdot 10^{-4}$	$1.4 \cdot 10^{-2}$	428.5 ± 40

2.1 Design and Assembly of the Reactor

In order to be able to control the chemical etching of the single-mode fibre, we designed and fabricated a reactor that enables the immobilization of the fibre in an HF-resistant structure, exposing only a given fibre length L to the acid.

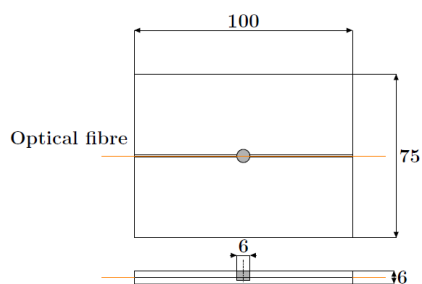


Figure 2: Scheme of the reactor designed for HF chemical etching of single-mode fibre. Heights represented in millimetres. The well depth is, approximately, 4.5 mm.

Figure 2 describes the size and shape of the fabricated reactor. In the assembly, 6 mm of the fibre is positioned in the place of the acid, while the rest of the fibre is isolated. The process followed for the fabrication comprises:

1. Drilling a 100×75×3 mm polymethylmethacrylate (PMMA) plate (Plexiglass®) with 6 mm diameter.
2. Locate another PMMA plate with the same dimensions below with an indent under the same 6 mm diameter hole as the top plate.
3. Placement of the optical fibre between both plates, having peeled the plastic coating of the fibre in the length to be etched. A small slot is marked in the PMMA to locate the SMF-28 fibre.
4. Both plates are sealed with Ethylene-vinyl acetate (EVA) plastic glue (Rapid®).
5. Measurement of the received power after transmission through the installed fibre (using the experimental setup depicted in Figure 1) before starting the chemical etching in order to verify that the fibre has not been damaged.

With the SMF-28 fibre located in the reactor we can start the chemical etching following the procedure described in the next section.

2.2 Chemical Etching of the Fibre

In this paper, we report the results obtained with two different methods for tapered fibre fabrication. In first place, we evaluate a chemical etching procedure performed at a single reaction rate (Bal et al., 2012). This procedure is very sensitive and difficult to control, so we present a novel method that controls the produced reaction in order to obtain a stable diameter reduction. This second fabrication method is presented with the intention of increasing the repeatability and automation of the process.

The main steps followed for the chemical etching and fabrication of the tapered fibre are:

1. Connection of the ECL laser to the input of the SMF-28 reactor and monitoring the optical power level at the fibre output using the experimental setup depicted before in Figure 1. In this experiment, the input power is set to -15 dBm (31.6 μ W).
2. Addition of 75 μ L HF 49.5 wt % in the reactor.
3. Power monitoring and extraction of the HF when the desired power level is reached.
4. Addition and extraction of 75 μ L of deionized water for removing of HF residue.
5. Neutralization of the acid in the reactor with 75 μ L of 5M NaOH. It should be noted that the chemical reaction between HF and NaOH is aggressive and forms NaF crystals that could damage the microfibre. For this reason, the HF residue should be minimum and the concentration is reduced in the previous step with deionized water.
6. Stabilization of the reactor with 75 μ L of 0.1M NaOH over 30 minutes. While the stabilization takes place, the power is also monitored as if the power continues decreasing means that the diameter is also decreasing.
7. Evaluation of the resulting fibre diameter by microscopy observation.

The power relation from Equation 5 is represented in Figure 3 from the experimental data obtained with the conventional chemical etching procedure. The received optical power level at the output of the fibre does not vary before 2800 s following the linear relation reported in (Haddock et al., 2003).

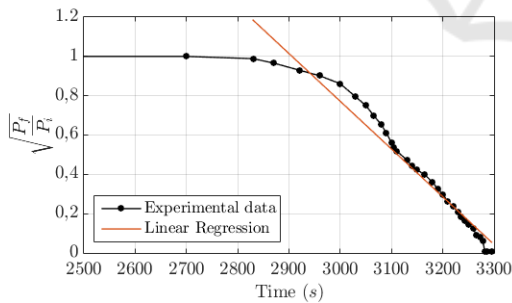


Figure 3: Experimental optical power levels measured using conventional chemical etching and linear regression with analytical expression $\sqrt{P_f / P_i} = 8.06 - 0.0024t$ and a coefficient of determination $R^2 = 0.9602$.

As it can be observed in Figure 3, the power fall is considerably fast and abrupt, making the procedure of acid extraction and neutralization complicated considering the security measures when dealing with HF acid. In this first experiment, due to the inability to extract the acid at the exact moment, the fibre was

completely degraded. For this reason, we propose to include an additional step between 2 a 3 adding some extra drops of water during the chemical reaction. This reduces the HF concentration in the reactor and therefore reduces the reaction rate (Ko et al., 2016) and the K parameter of Equation 5. This enables a more controllable and reproducible chemical etching. In this work, a water volume input control system depending on the rate of change of output power (dP_f/dt) was implemented as:

$$V_{H_2O} = V_i \cdot \rho_{HF} \cdot \left(\frac{C_0}{C_1} - 1 \right) \quad (6)$$

The direct relationship between P_f and [HF] is not known, but we know that dP_f/dt decrease in absolute value when [HF] is reduced. Thus, the control system decreases the concentration of acid proportionally to the increase of dP_f/dt over a desired value by adding a certain volume of water and extracting the same volume from the resulting solution. This reaction is represented mathematically in Equation 6 and Equation 7:

$$C_1 = C_0 - \left(\frac{dP_f}{dt} - \frac{dP_{desired}}{dt} \right) \cdot C_0 \quad (7)$$

where V_{H_2O} is the volume of water to be added, ρ_{HF} is the density of the HF acid and C_0 and C_1 are the initial and final concentrations of the solution, respectively. Following this approach, a reasonable value of variation rate of P_f is 1 μ W/s.

2.3 TFOBS Fabrication Results with Optically Controlled Etching

Figure 4 shows the experimental power variation measured with the optically controlled etching method as a function of the reaction time. In this research, eight tapered fibres samples were manufactured using manual control of [HF] as a function of the P_f variation, to ensure the reliability and repeatability of the method. The results depicted in Figure 4 correspond to TFOBS sample 7. We represented the three extra steps of V_{H_2O} addition to control the etching rate. In this case, the added volume was $V_{H_2O} = 75 \mu$ L. If we consider an automated control system for mass production, the added volume would depend on the increase of $|dP_f/dt|$.

Taking into account the K obtained from the linear regression and the duration of the etching, the procedure using the optically controlled etching is less abrupt as it can be observed in Figure 4. This

means that more time is available to perform the acid neutralization, but at the expense of longer etching time for the fabrication of the tapered fibre.

Figure 5 shows the images of the resulting tapered fibre taken with a digital microscope camera (Leica DFC420) of the 7th sample. The results with the eight samples obtained a final cladding diameter ranging from 10 μm to 40 μm, depending on the power ratio considered to stop the etching. Due to fibre contact with EVA, the resulting tapers were more likely non-adiabatic.

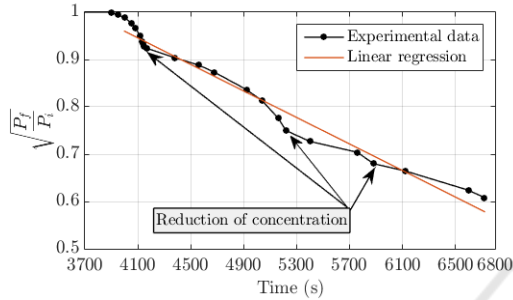


Figure 4: Experimental optical power levels measured using optically controlled chemical etching and linear regression with analytical expression $\sqrt{P_f/P_i} = 1.52 - 1.40 \cdot 10^{-4}t$ and a coefficient of determination $R^2 = 0.9754$.

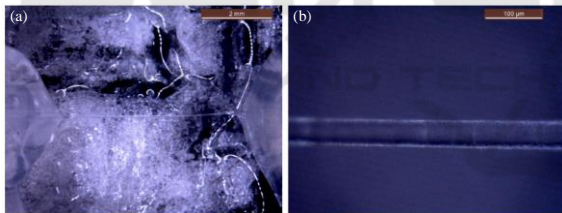


Figure 5: Microscope images of the 7th sample fabricated with the optically controlled etching: (a) the 5 mm length of the microfibre taper and (b) zoom of the microfibre.

3 TFOBS PERFORMANCE FOR LABEL-FREE GLUCOSE CONCENTRATION SENSING

Fibre optic tapers and microfibres generate a strong EF, making the optical transmission dependent on the refractive index of the medium (Polynkin et al., 2005). Especially in non-adiabatic optical fibres, but also in adiabatic depending on its characteristics, the fundamental mode (LP₀₁) propagated by a standard SMF-28 fibre is coupled to higher order modes, mainly LP₀₂ and LP₁₁, whose power distribution in the fibre core is displaced to the cladding (Zibai et

al., 2010). The velocity of propagation (β) of each mode depends on the effective refractive index of the medium (n_{eff}):

$$\beta = n_{eff} \cdot \frac{2\pi}{\lambda_0} \quad (8)$$

According to Equation 8, the β of the modes transmitted on the cladding depends on the n_{eff} of the external medium more than the modes transmitted in the core. This generates an offset, dependent to the medium, between the modes defined in Equation 9, that can be registered as a phase shift in the received signal (Yadav et al., 2014). The change of the medium also generates a intensity variation in the received signal according to Equation 10.

$$\Delta\phi = \Delta\beta \cdot L \rightarrow \Delta\phi = \Delta n_{eff} \cdot \frac{2\pi \cdot L}{\lambda_0} \quad (9)$$

$$I = I_1 + I_2 + 2\sqrt{I_1 I_2} \cdot \cos(\Delta\phi) \quad (10)$$

In addition to this, due to the taper's behaviour as a resonance cavity, the output signal exhibits quasi-periodic oscillations in the transmittance spectrum (Salceda-Delgado et al., 2012), whose spatial frequency also depends on the refractive index of the medium. This enables measuring experimentally three main optical parameters: intensity, phase shift and spatial period of the oscillatory signal, all of them correlated with the refractive index of the medium (Shi et al., 2012).

3.1 Glucose Sensing Simulation Study

In order to completely characterize the physical behaviour for the detection of glucose concentration, a simulation study was performed using COMSOL Multiphysics and MATLAB Optical Fibre Toolbox (Karapetyan, 2012). Figure 6 shows the simulated electric field generated in the microfibre considering a 15 μm cladding diameter and the transmission of first and second order modes at $\lambda = 1550$ nm.

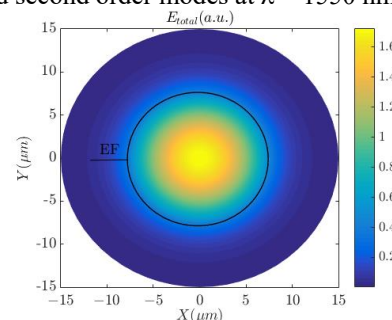


Figure 6: Simulated total electric field transverse plane propagated in a fibre with $D_f = 15$ μm cladding diameter.

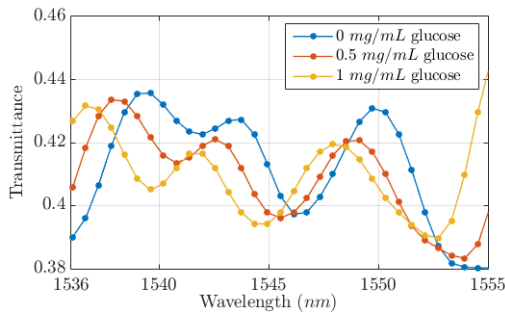


Figure 7: Transmittance between simulated results of the 2D biconical structure designed in COMSOL. Input signal implementing with LP₀₁ and LP₀₂ modes.

The simulation results indicate that the electric field intensity at 4 μm away from the cladding is approximately 10% of the mean intensity transmitted through the microfibre. Additionally, a 2D model of the TFOBS structure was programmed, where the index of refraction of the external medium was defined as a function of a glucose concentration in distilled water. A complete simulation study is performed considering 50 wavelength values between 1536 nm and 1555 nm with a parametric sweep of 50 glucose concentrations between 0 mg/mL and 50 mg/mL (Zibai et al., 2010). Figure 7 shows the transmittance values obtained for different glucose concentrations. Considering a fixed wavelength, we can observe the power decrease with the glucose concentration. The phase shift when the concentration of glucose in the medium changes can also be observed in Figure 7.

3.2 TFOBS Experimental Results for Glucose Concentration Sensing

Figure 8 shows the experimental setup implemented in the laboratory to evaluate the performance of the developed TFOBS for glucose concentration sensing. Ten glucose solutions between 0 mg/mL and 170 mg/mL in sterile saline, and 5 sodium chloride solutions between 0 mg/mL and 20 mg/mL in glucose 50 mg/mL solution were prepared with anhydrous glucose (99.7% pure), sterile saline solution (0.9%) and sodium chloride (99.6% pure). An external cavity laser (ECL) or a super-continuum laser (SCL) are used to measure the intensity or phase behaviour with different glucose concentrations. The received signal after the transmission through the TFOBS is measured with a power meter and an optical spectrum analyser (OSA, Advantest Q8384). Once the light source is stabilized, the optical signal is fed to the TFOBS using a VOA to set the input level to -21 dBm.

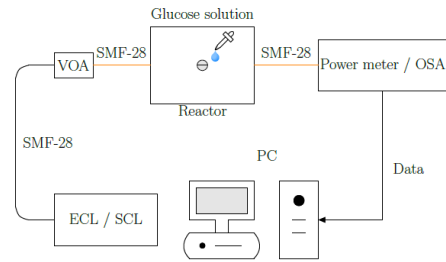


Figure 8: Experimental setup developed at the laboratory for the evaluation of the TFOBS intensity and phase variations for glucose concentration sensing.

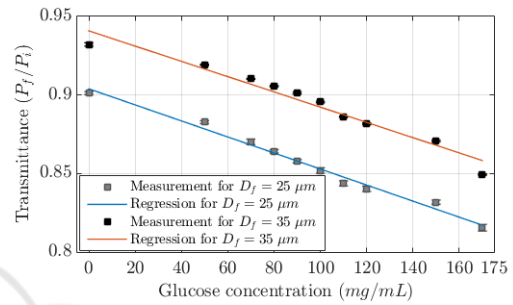


Figure 9: Measured transmittance and linear regression for different glucose concentrations in sterile saline solution.

Then, the target solutions with different glucose concentrations are applied to the TFOBS. After each measurement, the TFOBS is cleaned with deionized water 5 times before applying a new solution.

Figure 9 shows the measured transmittance and calculated linear regression obtained with TFOBS samples 5 and 7 fabricated with the proposed optically controlled etching method. The transmittance is defined as the ratio between the output power measured with an air sample and with a glucose solution. The difference between the measurements obtained with the different TFOBS samples correspond to a different final cladding diameter: 25 μm for 5th sample and 35 μm for 7th sample. It can be observed that the behaviour of the linear regression is similar despite the differences in diameter: the $D_f = 35 \mu\text{m}$ TFOBS (corresponding to the 7th sample) has an analytical regression defined by $T = 0.9413 - 4.89 \cdot 10^{-4}[G]$ with a coefficient of determination $R^2 = 0.9608$, while the TFOBS with $D_f = 25 \mu\text{m}$ (5th fabricated sample) corresponds to $T = 0.9039 - 5.10 \cdot 10^{-4}[G]$ with $R^2 = 0.9865$.

The sensitivity begins to increase considerably when approaching to the core diameter, but at the expenses of increasing also its fragility and the noise level in the measure. The sensitivity of the TFOBS with 35 μm cladding (7th sample) is calculated to be

$4.89 \cdot 10^{-4}$ in absolute value, with a limit of detection (LOD) by noise at 0.481 mg/mL.

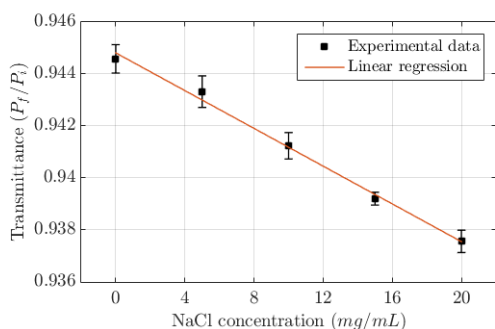


Figure 10: Mean, standard deviation and linear regression for NaCl concentrations in glucose 50 mg/mL measured with TFOBS with 25 μ m cladding (5th sample).

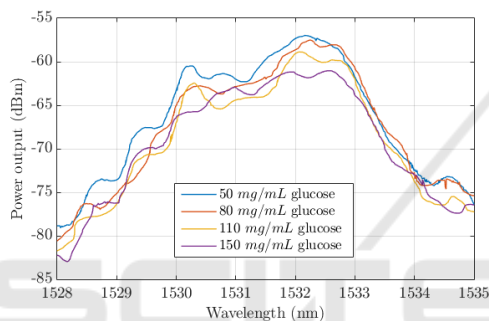


Figure 11: Received SCL spectrum measured with different glucose concentrations obtained with a TFOBS with 35 μ m cladding (7th sample). (0:01 nm resolution).

Figure 10 shows the mean, standard deviation and linear regression of the transmittance variation of the TFOBS with 25 μ m cladding (5th sample) for different NaCl concentrations in 50 mg/mL glucose. Due to the non-specific measurement of the refractive index, a variation in NaCl concentration also impacts on the resulting TFOBS transmittance.

To increase the TFOBS specificity, it would be necessary to immobilize a bioreceptor such as antibodies (Ruan et al., 2008) with a glucose conjugation (Liébana et al., 2016) or glucose oxidase enzyme (Khan et al., 2014), which could also be used as a labelled sensor because of GOx fluorescent performance (Klonoff, 2012). Figure 11 shows the experimental data obtained with TFOBS with 35 μ m cladding (7th sample) for different glucose concentrations in sterile saline solution. In this case, as depicted in Figure 8, a SCL generating a full width half maximum (FWHM) optical spectrum of 5 nm centred at 1532 nm wavelength is used as the light source to obtain the frequency response of the TFOBS. Figure 11 shows the variation of the

spectrum measured with the OSA when different glucose concentrations are applied to the TFOBS.

4 CONCLUSIONS

This paper proposes and evaluates experimentally an optically controlled etching method for the fabrication of single-mode TFOBS. Comparing the performance of the proposed method with single rate chemical etching, a more accurate design of the resulting tapered fibre is obtained with a controlled-rate etching, which improves the accuracy and repeatability of the fabrication. A reactor was designed to perform a secure chemical etching with HF acid. Also, the reliability of the output power monitoring and its correlation with the resulting diameter of the microfibre has been evaluated experimentally, confirming that it is a safe method for the chemical etching monitoring fulfilling the safety guidelines for HF handling.

Eight TFOBS samples with different final cladding diameters of the tapered fibre have been produced with the proposed optically controlled etching fabrication method and evaluated experimentally for the detection of glucose concentration. The TFOBS sensor comprising a tapered fibre with 35 μ m final cladding diameter obtained a sensibility of glucose concentration sensing of $4.89 \cdot 10^{-4}$ (mg/mL)⁻¹ in absolute value, with a LOD of 0.481 mg/mL. This is an acceptable sensing range for glucose concentration monitoring with a simple and low-cost implementation.

In this work, label-free glucose detection is evaluated. Specific glucose bioreceptors could be used to further improve the TFOBS specificity, and consequently, its sensitivity and LOD. The materials employed for the single-mode TFOBS fabrication are low-cost, which makes the process affordable and optimized for the fabrication of glucose concentration sensors. The proposed fabrication method could be implemented as an automated control system for mass production.

ACKNOWLEDGEMENTS

This research was supported in part by Spain National Plan MINECO/FEDER UE TEC2015-70858-C2-1-R XCORE and RTC-2014-2232-3 HIDRASENSE projects. M. Morant work was partly supported by UPV postdoc PAID-10-16 program. BIOFRACTIVE project with IIS La Fe is also acknowledged.

REFERENCES

- Abbadie, a., Hartmann, J. M., and Brunier, F. (2007). A review of different and promising defect etching techniques: from Si to Ge. *The Electrochemical Society A*, 10(1):3–19.
- Bal, H. K., Brodzeli, Z., Dragomir, N. M., Collins, S. F., and Sidirolou, F. (2012). Uniformly thinned optical fibers produced via HF etching with spectral and microscopic verification. *Applied optics*, 51(13):2282–2287.
- Baude, E. and Branco, P. (2013). Numerical study of tapered fiber optics as evanescent field sensors. *SBMO/IEEE MTT-S International Microwave & Optoelectronics Conference (IMOC)*, 1–5.
- Bosch, M. E., Jes'us, A., S'anchez, R., Rojas, F. S., and Ojeda, C. B. (2007). Recent development in optical fiber biosensors. *Sensors*, 7:797–859.
- Ferri, S., Kojima, K., and Sode, K. (2011). Review of glucose oxidases and glucose dehydrogenases: a bird's eye view of glucose sensing enzymes. *Diabetes Science and Technology*, 5(5):1068–1076.
- Fielding, A. J. and Davis, C. C. (2002). Tapered single-mode optical fiber evanescent coupling. *IEEE Photonics Technology Letters*, 14(1):53–55. G.
- Guo, Z. J., Boyter, C., Cohoon, G., Salik, E., and Lin, W.-J. (2011). Detection of botulinum neurotoxin by tapered fiber optic biosensor. *GSTF Journal of BioSciences* 1(1):36–42.
- Haddock, H. S., Shankar, P. M., and Mutharasan, R. (2003). Fabrication of biconical tapered optical fibers using hydrofluoric acid. *Materials Science and Engineering B: Solid-State Materials for Advanced Technology*.
- Karapetyan, K. (2012). *Single optical modal interferometer*. PhD thesis.
- Khan, A. Y., Noronha, S. B., and Bandyopadhyaya, R. (2014). Glucose oxidase enzyme immobilized porous silica for improved performance of a glucose biosensor. *Biochemical Engineering Journal*, 91:78–85.
- Klonoff, D. C. (2012). Overview of fluorescence glucose sensing: f Technology with a bright future. *Journal of Diabetes Science and Technology*, 6(6):1242–1250.
- Ko, S., Lee, J., Koo, J., Joo, B. S., Gu, M., and Lee, J. H. (2016). Chemical wet etching of an optical fiber using a hydrogen fluoride-free solution for a saturable absorber based on the evanescent field interaction. *Journal of Lightwave Technology*, 34(16):3776–3784.
- Leung, A., Shankar, P. M., and Mutharasan, R. (2008a). Label-free detection of DNA hybridization using gold-coated tapered fiber optic biosensors (TFOBS) in a flow cell at 1310 nm and 1550 nm. *Elsevier*, 131:640–645.
- Leung, A., Shankar, P. M., and Mutharasan, R. (2008b). Model protein detection using antibody-immobilized tapered fiber optic biosensors (TFOBS) in a flow cell at 1310 nm and 1550 nm. *Sensors and Actuators, B: Chemical*, 129(2):716–725.
- Liébana S, and Drago G.A. (2016). Bioconjugation and stabilisation of biomolecules in biosensors. *Essays in Biochemistry*, 60(1):59–68.
- Kenny, R. P., Birks, T. A, and Oakley, K. P. (1991). Control of optical fibre taper shape. *Electronics Letters*, 27.
- Polynkin, P., Polynkin, A., Peyghambarian, N., and Mansuripur, M. (2005). Evanescent field-based optical fiber sensing device for measuring the refractive index of liquids in microfluidic channels. *Optics Letters*, 30(11):1273–1275.
- Qiang, Z., Junyang, L., Yanling, Y., Libo, G., and Chenyang, X. (2014). Micro double tapered optical fiber sensors based on the evanescent field-effect and surface modification. *Optik*, 125(17):4614–4617.
- Qiu, H. W., Xu, S. C., Jiang, S. Z., Li, Z., Chen, P. X., Gao, S. S., Zhang, C., and Feng, D. J. (2015). Applied surface science a novel graphene-based tapered optical fiber sensor for glucose detection. *Elsevier*, 329:390–395.
- Ruan, Y., Foo, T. C., Warren-Smith, S., Hoffmann, P., Moore, R. C., Ebendorff-Heidepriem, H., and Monro, T. M. (2008). Antibody immobilization within glass microstructured fibers: a route to sensitive and selective biosensors. *Optics Express*, 16(22):18514–18523.
- Salceda-Delgado, G., Monzon-Hernandez, D., Martinez-Rios, a., Cardenas-Sevilla, G. a., and Villatoro, J. (2012). Optical microfiber mode interferometer for temperature-independent refractometric sensing. *Optics Letters*, 37(11):1974.
- Shi, J., Xiao, S., Yi, L., and Bi, M. (2012). A sensitivity-enhanced refractive index sensor using a single-mode thin-core fiber incorporating an abrupt taper. *Sensors*, 12(4), 4697–4705.
- World Health Organization (2016). *Diabetes Global Report*. Technical report.
- Yadav, T. K., Narayanaswamy, R., Abu Bakar, M. H., Kamil, Y. M., and Mahdi, M. A. (2014). Single mode tapered fiber-optic interferometer based refractive index sensor and its application to protein sensing. *Optics Express*, 22(19):22802.
- Zibaii, M. I., Latifi, H., Karami, M., Gholami, M., Hosseini, S. M., and Ghezelayagh, M. H. (2010). Non-adiabatic tapered optical fiber sensor for measuring the interaction between a-amino acids in aqueous carbohydrate solution. *Measurement Science and Technology*, 21(10):105801.